Analysis of the lateral dynamics of a vehicle and driver model running straight ahead

Fabio Della Rossa[ID], Gianpiero Mastinu

Abstract In this paper, we show that even an extremely simple nonlinear vehicle and driver model can show complex behaviors, like multi-stability and sensible dependence on the initial condition. The mechanical model of the car has two degrees of freedom, and the related equations of motion contain the nonlinear characteristics of the tires. The driver model is described by a single (nonlinear) equation, characterized by three parameters that describe how the driver steers the vehicle. Namely such parameters are the gain (steering angle per lateral deviation from desired path), the preview distance, and the reaction time delay. Bifurcation analysis is adopted to characterize straight ahead motion at different speeds, considering separately the two cases of understeering or oversteering cars. In the first case, we show that at suitable speeds the model can have three different attracting oscillating trajectories on which the system can work and that are reached due to different disturbances. In the second case, we confirm that instability arises if the forward speed is too high. The final results of the paper, bifurcation diagrams, can be used for many considerations critical both from the theoretical and from the practical viewpoints.

Keywords Vehicle system dynamics · Driver · Multi-stability · Bifurcation analysis · Nonlinear systems

Received: 28 October 2016
Accepted: 13 March 2017
Published online: 24 March 2017

F. Della Rossa (✉) · G. Mastinu
Politecnico di Milano, Piazza Leonardo da Vinci 32, Milan, Italy
e-mail: fabio.dellarossa@polimi.it

1 Introduction

Even if straight ahead motion is the most frequent running condition, accounting for cars 98% of the travelled distance, the literature devoted to such a topic, looking in particular to the arising nonlinear phenomena, is far from be completed [1–5]. Unexpected hard lateral disturbances to the vehicle are one of the most important causes of accident, so that in Europe a number of tracks exist with the aim to train drivers in coping such phenomena [6–8]. In particular, it is important to understand not only how the vehicle behaves (i.e., if the vehicle can or cannot maintain a straight line trajectory), but also how drivers react in order to return to the desired straight trajectory they have to follow. In fact, vehicle–driver interaction, intrinsically part of the same system (the problem can be naturally recasted as a human-in-the-loop system), dramatically influences the overall behavior of the system. In this paper, we propose to analyze both the model of the vehicle and the vehicle + driver model.

In the literature, mathematical modeling of vehicle dynamics is often carried out looking at linear models [9–20], while only few papers and almost no textbooks deal in-depth with the analysis of nonlinear car models [3–5]. It is known that understeering vehicles can recover straight ahead running condition independently from the forward velocity (for small disturbances), while oversteering vehicles generically have a threshold speed after which even an infinitesimal disturbance causes the vehicle to miss the aimed trajectory.

These studies however analyze vehicle stability using local systems coordinates (on the vehicle itself), and therefore cannot cope with the real cases in which a particular—straight or bend—trajectory should be followed by a human or autonomous driver. In this paper, we gather some of the results given in [3,5,21] (referring only to straight ahead running condition), highlighting that nonlinear dynamical phenomena (like persistent periodic oscillations and sensible dependence on initial conditions) can arise even assuming the simplest driver model.

The paper is organized as follows. First we introduce and validate the system models of the car and of the driver, depending on the two main tire characteristics we already discussed (understeering and oversteering vehicles). Then we analyze what models predict, referring only to straight ahead motion. The tool used for this analysis is bifurcation theory [22–24]. Bifurcation theory is proposed because it is able to obtain global information about the system dynamics (e.g., the presence of other attractors, robustness, shape of the basin of attraction, …) looking at local phenomena (stability loss of a specific attractor). We therefore discuss the obtained results and propose directions for further research.

2 System model

In this section, we propose two mathematical models, one for the vehicle and one for the car + driver systems. The models we propose are as simple as possible, they contain only the essential characteristics needed for the description of both vehicle stability and the driver action to follow a given path. They are simple enough to allow an in-depth analysis. More complex (and more realistic) models can be proposed, but their analysis could be cumbersome. Validations of the simple proposed models are produced in the next section, showing that although the simplification hypotheses are strict, the models reproduce sufficiently well the actual vehicle and car + driver behaviors.

2.1 Vehicle model

The vehicle mechanical model analyzed in this paper is the well-known two degrees of freedom *single-track* model [3,9,11,25,26] shown in the left panel of Fig. 1. To obtain such a simplified model, the main assumptions are:

- the forward speed u is constant or varies much slower than the lateral velocity v of the vehicle;
- the center of gravity lies at the ground level;
- the vehicle body is modeled referring to its longitudinal axis;
- the resultant of the forces acting at the front and rear axles is applied at the centers of the axles;
- the slip angles α_i, $i = 1, 2$, and the steering angle δ (see Fig. 1) are small;
- no longitudinal forces are acting at the wheels (i.e., we neglect F_{x_1} and F_{x_2} depicted in Fig. 1).

Under the above hypothesis, the equations of motion with respect to the reference system of the vehicle read

$$\begin{aligned} m(\dot{v} + ur) &= F_{y_1}(v, r) + F_{y_2}(v, r) \\ I_z \dot{r} &= F_{y_1}(v, r)\, a - F_{y_2}(v, r)\, b \end{aligned} \tag{1a}$$

where dots stand for time-derivative, u and v are the longitudinal and lateral speeds, respectively, r is the yaw rate, subscripts 1 and 2 refer, respectively, to the front and rear axle, F_{y_i} is the lateral force on the i^{th} axle, m is the vehicle mass, a and b are the distances, respectively, of the front and the rear axle centers from the vehicle's center of mass, I_z is the moment of inertia of the vehicle around the vertical axis at the center of gravity. The front and rear slip angles can be obtained through the following equations:

$$-\alpha_2 = (v - rb)/u \qquad \delta - \alpha_1 = (v + ra)/u. \tag{1b}$$

The nonlinear dynamics of the model is embedded in the reaction functions of the tires [3,9]. Such lateral forces $F_{y_i}(\alpha_i)$ $(i = 1, 2)$ can be expressed as functions of the slip angles α_i [9] and are highly nonlinear. They typically saturate, i.e., lateral forces stop increasing if slip angles get high, as depicted in the right panel of Fig. 1. These nonlinear functions can have very different shapes, depending on tire size, tire pressure, tire temperature and wear, car center of gravity location, car mass, suspension kinematics, driving axle, torque distribution between the two wheels of the same axle, … (for a comprehensive description see [10]). The vehicle model behavior critically depends on these nonlinear functions [3]. In this paper, we analyze only two simple cases (monotonically increasing, not intersecting characteristics, i.e., the ones depicted in the right panel of Fig. 1) and we switch between understeering

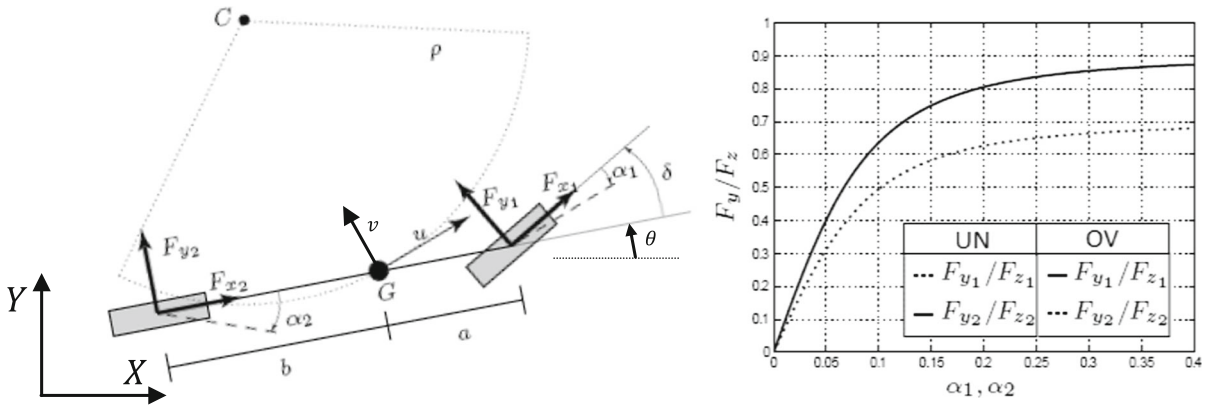

Fig. 1 *Left panel* representation of the single-track model. *Right panel* tire characteristics of the analyzed vehicles

Table 1 Considered vehicle and tire parameters

Vehicle		Front tire			Rear tire		
Mass m	950 kg		UN	OV		UN	OV
Principal inertia moment I_z	1100 kg m^2	B_1	10	10	B_2	10	10
Wheelbase l	2.46 m	C_1	1	1	C_2	1	1
a	0.95 m	E_1	0	0	E_2	0	0
b	1.51 m	μ_1	0.9	0.7	μ_2	0.7	0.9

(UN) or oversteering (OV) vehicles simply switching the front with the rear tires nonlinear functions. The analytic expression of those functions, known as *magic formulae* [9] is:

$$F_{y_i}(\alpha_i) = D_i \sin(C_i \arctan(B_i\alpha_i - E_i(B_i\alpha_i - \arctan(B_i\alpha_i)))) \quad (1c)$$

where $D_1 = \mu_1 (mg/l)\, b$, $D_2 = \mu_2 (mg/l)\, a$, μ_1 and μ_2 are the friction coefficients, while parameters B_i, C_i, E_i, $(i = 1, 2)$ shape the nonlinear functions. The parameter set can be divided into three subsets: the vehicle parameters $(m, I_z, a, b, l = a + b)$, the tire parameters $(\mu_i, B_i, C_i, E_i, i = 1, 2)$, and the parameters (u, δ) which represent the running conditions (Table 1).

The equilibrium of model (1) (no driver control) is represented by $(v, r) = (0, 0)$ and refers to a straight ahead running condition; the vehicle is running ahead on an undefined straight line. After a disturbance, if the system (without any control) comes back to the equilibrium, the straight line on which the vehicle runs is virtually different, both in slope and in position. If one wants to cope with the real case in which a driver must follow a specific straight trajectory (say, follow a line $Y = \tan\theta X$, where θ is the angle between the straight trajectory and the X axis, see Fig. 1), the model's reference system cannot be on the vehicle: We can always set, without losing generality, $\theta = 0$. In this case, we can assume that $\dot{X} \gg \dot{Y}$ (and therefore $u \sim \dot{X}$). Under this hypothesis, model (1) can be rewritten as [13,14,21]

$$\begin{aligned} m\,\ddot{Y} &= F_{y_1}(\theta, \dot{\theta}, Y) + F_{y_2}(\theta, \dot{\theta}, Y) \\ I_z\,\ddot{\theta} &= F_{y_1}(\theta, \dot{\theta}, Y)\, a - F_{y_2}(\theta, \dot{\theta}, Y)\, b \end{aligned} \quad (2a)$$

where the double dots stand for second time-derivative of the vertical position and the trajectory angle, while the slip angles should be shifted taking into account the (nonstationary) trajectory's slope, i.e.,

$$\theta - \alpha_2 = \frac{\dot{Y} - b\dot{\theta}}{u}, \quad \delta + \theta - \alpha_1 = \frac{\dot{Y} + a\,\dot{\theta}}{u} \quad (2b)$$

Note that the obtained model has now three state variables, namely $(\dot{Y}, \theta, \dot{\theta})$.

2.2 Driver model

We derive the simplest possible driver model, inspired to what was proposed in [4,5,10,11,21,27,30]. In this case, the model we analyze is the well-known *path follower* [10]. Summarizing its derivation, we first assume that the driver inside the car is able to see a point L forward beyond the current position of the vehicle and, exploiting such a point, he/she is able to estimate the deviation of the future position of the vehicle with respect to a reference path $(X_{\text{ref}},\ Y_{\text{ref}})$

$$\boldsymbol{e} = \begin{pmatrix} X \\ Y \end{pmatrix} + L \begin{pmatrix} \cos\theta \\ \sin\theta \end{pmatrix} - \begin{pmatrix} X_{\text{ref}} \\ Y_{\text{ref}} \end{pmatrix}$$

(note that, in general, $\boldsymbol{e}$ is a two-dimensional vector) and that the driver reacts with a gain $\boldsymbol{k}_p$ to this error with a delay τ_r, i.e.,

$$\delta\,(t+\tau_r) = \boldsymbol{k}_p\,\boldsymbol{e}\,(t)\,. \tag{3a}$$

Since we want to analyze only the straight ahead running, at steady state we can use a reference system in which X_{ref} can assume any value, while Y_{ref} has a precise constant value. We then assume that the driver has a delay in his/her reaction, and that it is possible to approximate this delay with the linear term of its Taylor expansion (this approximation is acceptable since the frequency at which a human can vary the steering angle does not exceed 3 Hz). So the final model of the driver simplifies to the differential equation:

$$\tau_r\,\dot{\delta} = -\delta + h(Y + L\sin(\theta) - Y_{\text{ref}}). \tag{3b}$$

The path follower is the simplest driver model. However, it is quite common to consider the reaction of the driver not only proportional to the error, but also considering how the error is changing (derivative feedback) [10]. In this case, equations (3) become

$$\begin{aligned} \delta\,(t+\tau_r) &= h\,\boldsymbol{e}(t) + k_{\text{d}}\,\dot{\boldsymbol{e}}(t) \\ \tau_r\,\dot{\delta} &= -\delta + k_p(Y + L\sin(\theta) - Y_{\text{ref}}) \\ &\quad + k_{\text{d}}(\dot{Y} + L\dot{\theta}\cos\theta). \end{aligned} \tag{4}$$

In this paper, we first analyze an autonomous driver (3), and then we will homotopically increase the derivative gain k_{d} in order to understand the effect of a more human-like driving behavior. The driver parameters used in the following for the analysis are taken from the literature (see, e.g., [4,5,11,21,27]) and are $\tau_r = 0.2\,\text{s}$, $k_p = 0.02\,\frac{\text{rad}}{\text{s}}$, $L = 12\,\text{m}$. Note that human drivers are able to adapt their parameters to maintain stability, or change their parameters in different driving conditions: Also in this case, we assume that driver parameters change slower than the lateral dynamics of the vehicle (and so we assume they are constant at constant forward speed u).

2.3 Car + driver model

We now couple the vehicle and the driver models to obtain a human-in-the-loop system. Since in this paper, we are only interested in the lateral dynamics, we assume that the driver cannot change his/her forward speed u (that will be treated as a parameter), while the steering angle δ is changed according to model (3) or (4). The complete model has five variables $(Y, \dot{Y}, \theta, \dot{\theta}, \delta)$ and reads

$$\begin{aligned} m\,\ddot{Y} &= F_{y_1}(\theta,\dot{\theta},Y) + F_{y_2}(\theta,\dot{\theta},Y) \\ I_z\,\ddot{\theta} &= F_{y_1}(\theta,\dot{\theta},Y)\,a + F_{y_2}(\theta,\dot{\theta},Y)\,b \\ \tau_r\,\dot{\delta} &= -\delta + h(Y + L\,sin(\theta) - Y_{\text{ref}}). \end{aligned} \tag{5}$$

This could be the case of an autonomous path follower. Referring to a more human-like behavior, we write

$$\begin{aligned} m\,\ddot{Y} &= F_{y_1}(\theta,\dot{\theta},Y) + F_{y_2}(\theta,\dot{\theta},Y) \\ I_z\ddot{\theta} &= F_{y_1}(\theta,\dot{\theta},Y)\,a + F_{y_2}(\theta,\dot{\theta},Y)\,b \\ \tau_r\,\dot{\delta} &= -\delta + h(Y + L\sin(\theta) - Y_{\text{ref}}) \\ &\quad + k_{\text{d}}(\dot{Y} + L\dot{\theta}\cos\theta). \end{aligned} \tag{5a}$$

The desired equilibrium of the model, $\left[Y, \dot{Y}, \theta, \dot{\theta}, \delta\right] = [Y_{\text{ref}}, 0, 0, 0, 0]$, represents a driver that follows a precise straight line trajectory with increasing abscissa (with velocity $\dot{X} = u$) and constant ordinate $Y = Y_{\text{ref}}$.

3 Validation

Two different validations of the simple models introduced in the previous section have been performed. The first validation is reported in the top panel of Fig. 2 and refers to a car running on a race track (for more details see [5]).

The second validation refers to tests performed at the ACI test track in Milan (Lainate), Italy. A severe yaw vehicle motion is excited by a kick-plate acting at the rear axle of the car at a certain time instant as the car is running straight ahead. The driver is heavily involved in controlling the yaw motion, to avoid

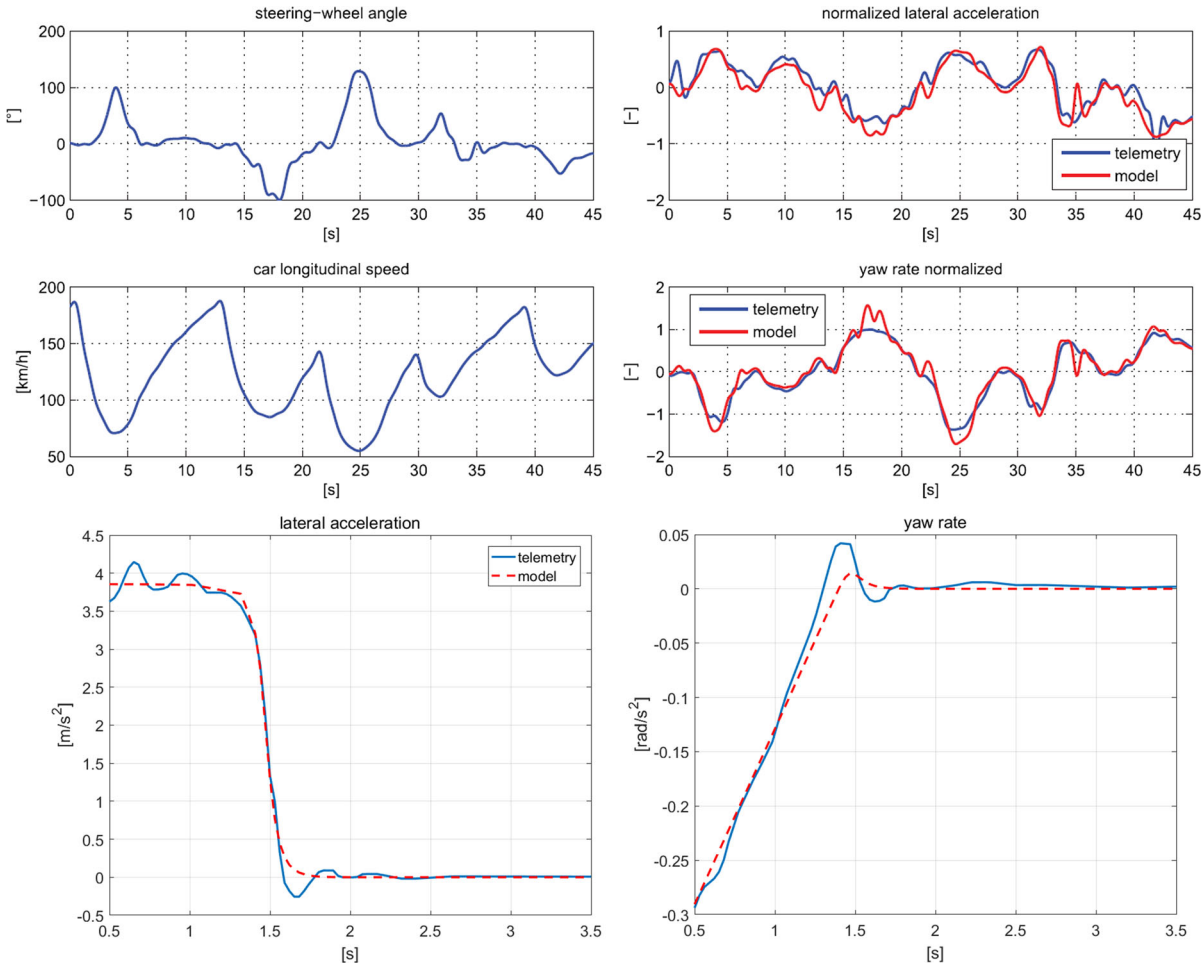

Fig. 2 Validation of system model (1) (*top panels*), and driver model (3) (*bottom panels*). Adapted from [5,21]

a complete spin. Driver parameters are then estimated through a nonlinear optimization algorithm. The results of this experiment are reported in the bottom panel of Fig. 2 (for more details see [21]). The mathematical models are implemented in MATLAB/Simulink: With these validations, we show that even the simple models we proposed can reasonably handle real data (the error that is found is not too high).

4 Fixed steering angle model analysis

The easiest (but not the only!) way for a vehicle to go straight ahead is with the steering angle fixed at $\delta = 0$. In this case, we can analyze model (1) looking at the stability of the trivial equilibrium $(v, r) = (0, 0)$ for different values of forward speed u. The linearized analysis [9–11] says that in the UN case, the equilibrium is always stable, while for the OV case, a maximum velocity exists ($u^P = 99.3$km/h in our case) at which the equilibrium becomes unstable: This qualitative change is called *bifurcation*. Bifurcation theory [3,24,25] allows us to analyze the influence of nonlinear terms of the model locally with respect to the bifurcation point. We can classify that point as a *catastrophic pitchfork bifurcation point,* discovering that two saddle equilibria, whose stable manifolds, before the bifurcation, limit the basin of attraction of the stable equilibrium, and then they collide and disappear at the bifurcation. By means of a *continuation algorithm* [22,23], it is possible to summarize the obtained results in Fig. 3, where the possible asymptotic regimes (stable—solid and unstable—dashed) are shown in the phase space

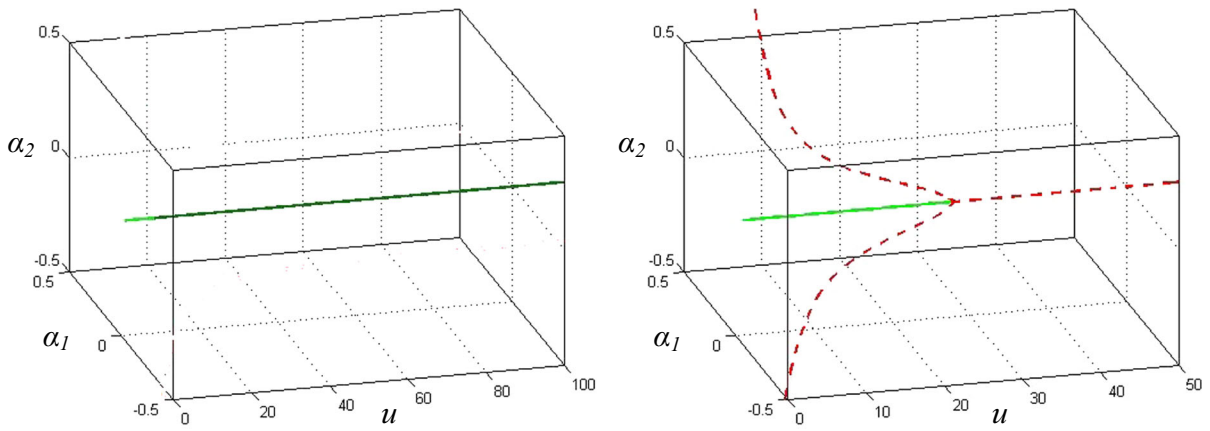

Fig. 3 Bifurcation diagrams of model (1) for the UN (*left*) and the OV (*right*) tire nonlinear functions in Fig. 1. *Solid line* stable equilibria. *Dashed lines* unstable equilibria

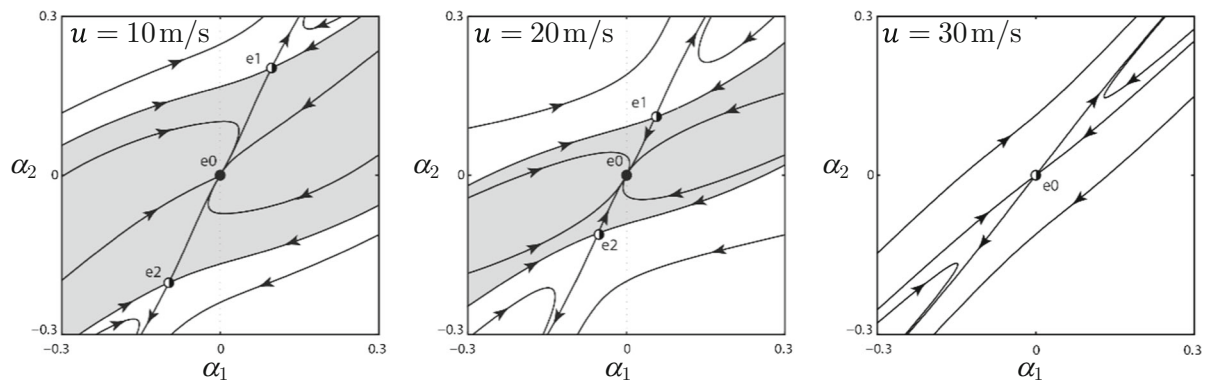

Fig. 4 Three different state portraits of model (1) with OV tire characteristics

(α_1, α_2) for different values of the parameter u. In the left panel, the UN case is shown: As expected, no other equilibria are present, and the trivial equilibrium is globally stable. In the right panel, the OV case is shown: In this case, three equilibria are present if $u < u^P$, the trivial one is stable while the other two are unstable (saddles). If u approaches the bifurcation value, the two unstable equilibria approach the stable one, and then they collide and disappear. After the bifurcation, the trivial equilibrium becomes unstable. To better understand this phenomenon, the phase space of this last case is shown in Fig. 4 for three increasing values of u. Note how the stable manifold of the saddles (e1 and e2 in the figure) delimit the basin of attraction (gray in the figure) of the 0 equilibrium (e0 in the figure). Approaching the catastrophic pitchfork bifurcation, the basin of attraction of the stable equilibrium shrinks, and even a small disturbance can cause a stability loss, a typical issue of catastrophic bifurcations.

5 Car + driver model analysis

The analysis presented in the previous section can be performed for the car + driver model (5). A projection in the (Y, θ, u) subspace of the results of such an analysis is presented in Fig. 5.

On the left panel, the case with an understeering car (UN) is shown. It is possible to note immediately, as previously discussed, how the presence of a driver and the need of targeting a particular trajectory dramatically changes the final expected behavior.

As a first remark, we note that introducing the driver's dynamic (i.e., control action) makes the straight

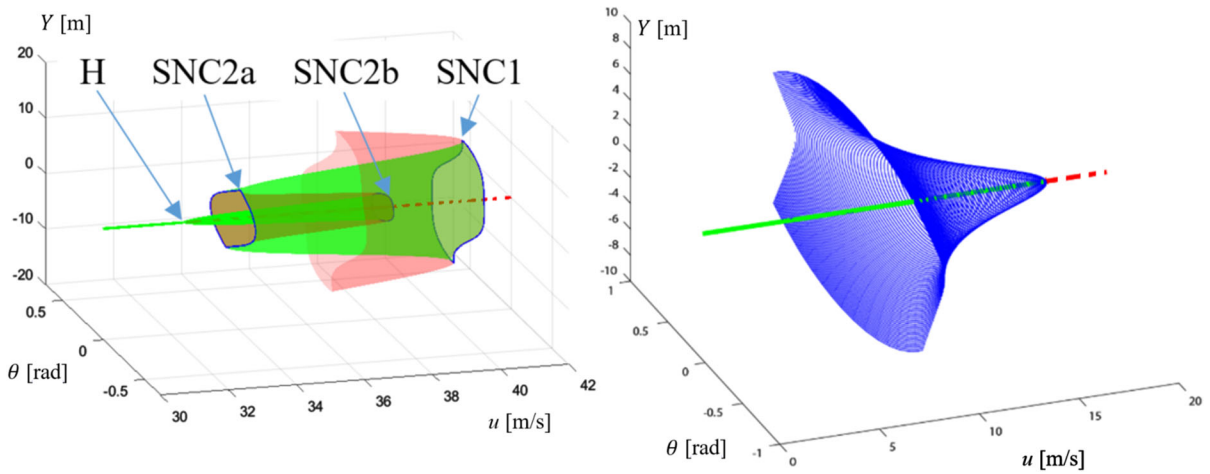

Fig. 5 Bifurcation diagrams of model (5) for the UN (*left*) and the OV (*right*) cases

ahead running condition unstable if the forward speed $u > u^H = 32.4$ m/s, at which a non-catastrophic Hopf bifurcation occurs. Being non-catastrophic, it means that the basin of attraction of the bifurcating solution is unbounded before the bifurcation, while after the bifurcation, a stable limit cycle substitutes the previous stable solution, with an amplitude that vanishes at the bifurcation point. This means that the driver who slowly increases the forward speed can realize a smooth loss of stability without violent dynamics, since initially the trajectory simply wiggles around the target (and comes back to the target if u is reduced). Even if the forward speed is further increased, the amplitude of the oscillations remains quite small (it starts from zero at 32.4 m/s and will reach about 0.5 m at 36 m/s), while the period is about 10 s, i.e., the frequency is about 0.1 Hz (these last two data cannot be seen in Fig. 5). At $u = 33.8$ m/s a saddle-node bifurcation of limit cycles occurs (SNC2a in Fig. 5). If $33.8 < u < 38.2$ m/s the model predicts two possible asymptotic behaviors, actually there are two stable limit cycles, one with big amplitude (around 7m, with steering angles that oscillates with amplitude around 6°), and one with small amplitude (around 1.5m, with amplitude of the corresponding steering angles around 1.5°). Reaching one or the other limit cycle depends on the initial disturbance (i.e., initial condition). After a small disturbance, the driver can keep the small amplitude limit cycle, and on the contrary after a big disturbance, the driver would be forced to cope with the biggest limit cycle. At $u = 38.2$ m/s, another saddle-node bifurcation of limit cycles occurs (SNC2b in Fig. 5), where the small amplitude limit cycle disappears and the big amplitude limit cycle is the only viable attractor. At $u = 44$ m/s, another saddle-node bifurcation of limit cycle occurs, and crashes (i.e., violent dynamics) cannot be avoided. Note that while all the trajectories can virtually be produced by the driver, only the ones with lowest amplitude can effectively be attained, since actual oscillations would be smaller than the street width. Attractor multiplicity reveals the fragility of those situations that easily lead to tragedy.

The right panel of Fig. 5 shows the bifurcation analysis performed for the oversteering case (OV). In this case, the behavior of model (5) matches with the behavior of model (1) depicted in Fig. 3 (right panel): At $u^H = 17$ m/s, a catastrophic Hopf bifurcation occurs, and the stability of the straight ahead running condition (obviously stable for forward speed sufficiently small) is lost. Notice that in this case, the Hopf bifurcation is catastrophic, and thus disturbances cannot be absorbed by the system if they are sufficiently big, and the amplitude of dangerous disturbances vanishes approaching the bifurcation, i.e., stability can be lost even for $u < u^H$ due to a finite disturbance.

Bifurcation analysis can be used not only to partition the parameter space into regions in which the system qualitatively behaves in the same way, but also to determine the regions in the parameter space in which the stationary regime has a sufficiently large basin of attraction, i.e., it is the only asymptotically stable regime (global stability) or, alternatively, large disturbances are

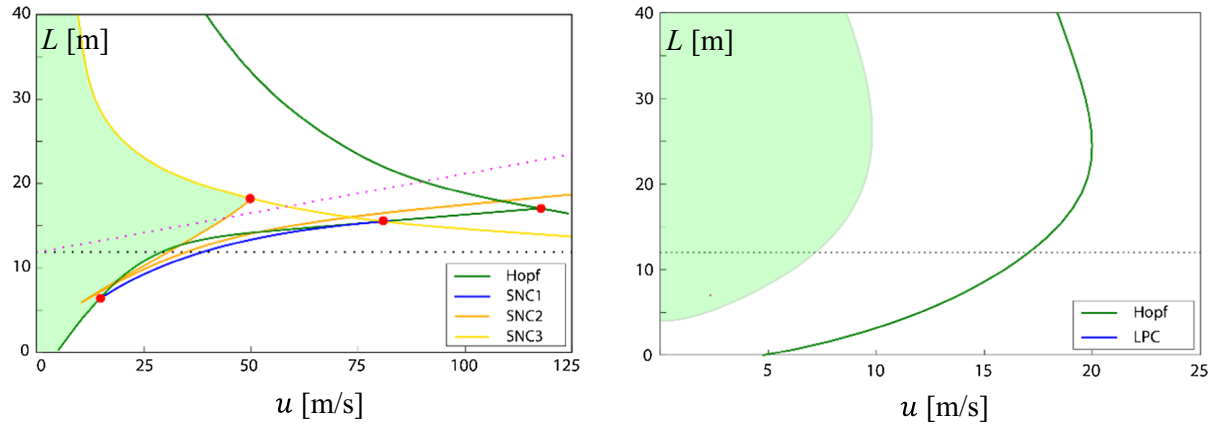

Fig. 6 Bifurcation diagrams in the (u, L) parameter space of model (5) for the UN (*left*) and the OV (*right*) cases

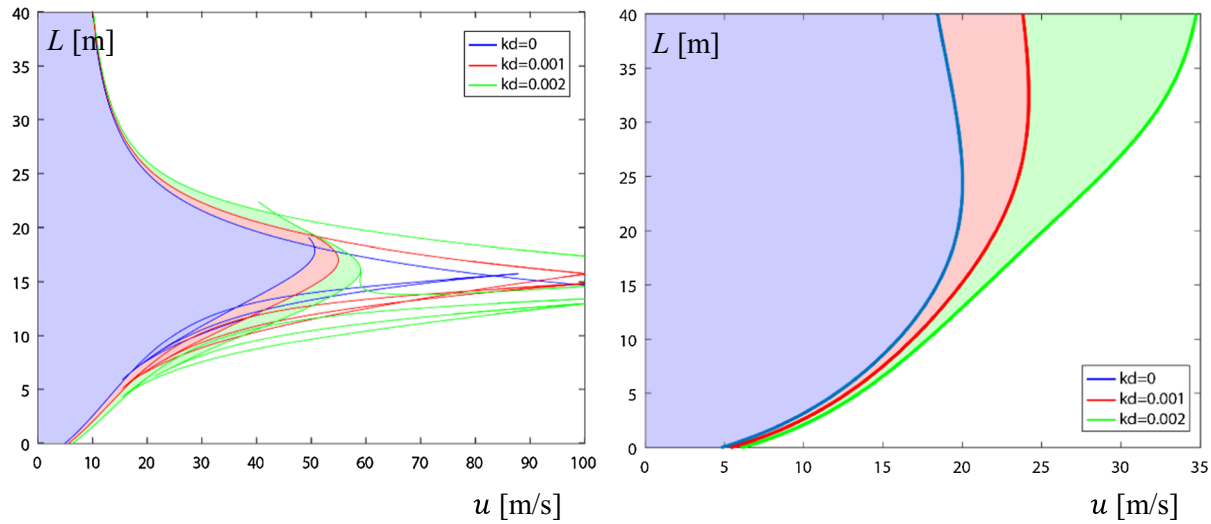

Fig. 7 Bifurcation diagrams of model (5a) for different values of k_d. *Left panel* UN case. *Right panel* OV case

absorbed by the system. The results of the addressed bifurcation analyses are shown in Fig. 6. Two parameters are considered, u, characterizing the running condition, and L qualifying the driver.

In the left panel of Fig. 6, the UN case is analyzed. The curves plotted are the bifurcation curves, i.e., the parameters combination at which one of the bifurcations we have described occurs. Note that the result we have discussed in Fig. 5 can be seen again following the black dotted line in Fig. 6. First, when $u = 32.4$ m/s, the green Hopf bifurcation curve is crossed. Then, the orange SNC2 bifurcation is crossed twice, and finally the blue SNC1 curve is crossed. The shaded area of the diagram that we will call the *stable domain* represents the parameter settings in which the car + driver straight ahead running condition can be recovered even after a big disturbance in the position Y ($\sim$10 m). Notice that this analysis suffers from the fact that even milder disturbances can trigger instability, if not only the position but also other state variables are considered [28]. Nevertheless, the stable domain can give a good idea of the region in which the system is robust. The bifurcation diagrams in Fig. 6 can be used to fast analyze other cases: For example, with a small preview distance (e.g., $L = 6$ m) only a Hopf bifurcation would occur, even if in this case, the bifurcation is catastrophic. Or again, since the preview distance L may depend on speed u [4,10,11], we can set $L = L(u)$ and follow a specific

line on the bifurcation diagram to see which bifurcations occurs. For example, the sloped straight line featuring $L = ku$ is depicted (pink dotted). In this case, the sequence of bifurcations is quite different with respect to the one described in Fig. 5: Two saddle-nodes of limit cycles bifurcations occur before the Hopf bifurcation.

In the right panel of Fig. 6, the OV case is reported. Only a catastrophic Hopf bifurcation curve occurs, at which, as seen in Fig. 5, an unstable limit cycle shrinks on the desired asymptotic condition. As already said, since the Hopf bifurcation is catastrophic, the basin of attraction of the straight ahead running condition is bounded by (the stable manifold of) the unstable limit cycle involved in the bifurcation: This is why by increasing u we quit the stable domain (shaded in the figure) much before we lose stability. The dotted horizontal line refers to $L = 12$m, i.e., to the case analyzed in Fig. 5.

The last question we want to answer in this paper is whether a more "human like" driving behavior improves or worsens the obtained results. This can be done analyzing model (5a) and reproducing the diagrams in Fig. 6 for increasing values of k_d. The result of this simulation is reported in Fig. 7. In both cases, adding derivative feedback enlarges the stability domain.

6 Conclusion and discussion

In this paper, we have analyzed simple car and car + driver nonlinear models in order to study straight ahead running at different forward velocities. The novelty of the paper refers not only on body-fixed [3,5,29], but also on ground-fixed local coordinates, thus obtaining a model that can effectively reproduce the driver behavior. We have synthesized the stability and the robustness of the desired asymptotic behavior by means of bifurcation diagrams. Such diagrams can be used to understand and quantify the safety level associated with a particular car and driver control (in terms of their distance to the stability region boundary).

A number of often unreferenced (but actual) behaviors have been described by exploiting the simple models used. Limit cycles and the sudden loss of stability are all described in a comprehensive framework.

A straightforward comparison between understeering and oversteering vehicles has been carried out, remarking the common experience that oversteering vehicles are quite more dangerous than understeering ones. This can be seen looking both at the parameter values at which the loss of stability occurs and at the differences in the reshaping of the basin of attraction (and, thus, the ability of the system to absorb disturbances) for increasing velocity.

The results of the paper fully agree with practice. Actually it is well known that the driver may make a vehicle that is inherently stable unstable. Also, it is well known from practice that a skilled driver may make an unstable vehicle stable.

The proposed analysis complements and must be taken into considerations for all the studies on traffic flow behaviors. In particular, many studies (also based on bifurcation theory, see, e.g., [31–33]) consider how the traffic flow is affected depending on different driver's characteristics, without checking the lateral stability of each driven vehicle.

The influence of a number of vehicle parameters (namely, the speed, the nonlinear functions describing tire forces, the driver preview distance, the driver control delay and the driver steering gain) on vehicle stability has been highlighted. Although an experimental validation of the obtained results is still to be completed, the paper addresses unreferenced issues on vehicle driver behavior that can be useful to vehicle designers, chassis control engineers, traffic psychologist, and infrastructure planners.

References

1. Andrzejewski, R., Awrejcewicz, J.: Nonlinear Dynamics of a Wheeled Vehicle, vol. 10. Springer Science & Business Media, Berlin (2006)
2. Apel, A., Mitschke, M.: Adjusting vehicle characteristics by means of driver models. Int. J. Veh. Des. **18**, 583–596 (1997)
3. Della Rossa, F., Mastinu, G., Piccardi, C.: Bifurcation analysis of an automobile model negotiating a curve. Veh. Syst. Dyn. **50**, 1539–1562 (2012)
4. Plochl, M., Edelmann, J.: Driver models in automobile dynamics application. Veh. Syst. Dyn. **45**(7–8), 699–741 (2007)
5. Della Rossa, F., Gobbi, M., Mastinu, G., Piccardi, C., Previati, G.: Bifurcation analysis of a car and driver model. Veh. Syst. Dyn. **52**, 142–156 (2014)
6. http://www.hytronics.at/
7. http://www.vallelunga.it/
8. Lozia, Z.: Modelling and simulation of a disturbance to the motion of a motor vehicle entering a skid pad as used for tests at driver improvement centres. In: Archiwum Motoryzacji vol. 69 PIMOT, Warsaw University of Technology (2015)

9. Pacejka, H.: Tire and Vehicle Dynamics, 2nd edn. Elsevier, Amsterdam (2006)
10. Mastinu, G., Plöchl, M.: Road and Off-Road Vehicle System Dynamics Handbook. CRC, Boca Raton (2014)
11. Mitschke, M., Wallentowitz, H.: Dynamik der Kraftfahrzeuge, 4th edn. Springer, Berlin (2004)
12. Gillespie T.D.: Fundamentals of vehicle dynamics. SAE International (1992)
13. Abe, M.: Vehicle Handling Dynamics. Elsevier, Oxford (2015)
14. Jazar, R.N.: Vehicle Dynamics: Theory and Application. Springer, Berlin (2008)
15. Andrzejewski, R., Awrejcewicz, J.: Nonlinear Dynamics of a Wheeled Vehicle. Springer, Berlin (2005)
16. Guiggiani, M.: The Science of Vehicle Dynamics. Springer, Berlin (2013)
17. Genta, G.: The Automotive Chassis. Springer, Berlin (2016)
18. Reimpell, J., et al.: The Automotive Chassis. Butterworth-Heineman, Oxford (2001)
19. Crolla, D.: Encyclopedia of Automotive Engineering. Wiley, Chichester (2015)
20. Dixon, J.: Tires. Suspension and Handling. Society of Automotive Engineers, Warrendale (1996)
21. Della Rossa, F., Sukharev, O., Mastinu, G.: Straight ahead running of a nonlinear car and driver model. In: AVEC, Munich (2016)
22. Dhooge, A., Govaerts, W., Kuznetsov, Y.A.: MATCONT: a MATLAB package for numerical bifurcation analysis of ODEs. ACM Trans. Math. Softw. **29**, 141–164 (2003)
23. Doedel, E.J., Champneys, A.R., Fairgrieve, T., et al.: AUTO-07P: continuation and bifurcation software for ordinary differential equations. Concordia University, Montreal (2007)
24. Kuznetsov, YuA: Elements of Applied Bifurcation Theory. Springer, New York (2004)
25. Mastinu, G., Della Rossa, F., Piccardi, C.: Nonlinear dynamics of a road vehicle running into a curve. Appl. Chaos Nonlinear Dyn. Sci. Eng. **2**, 125–153 (2012)
26. Pacejka, H.: Simplified analysis of steady-state turning. Veh. Syst. Dyn. **21**, 269–296 (1973)
27. Gobbi, M., Mastinu, G., Previati, G., De Filippi, R., Lunetta, I., Moscatelli, D.: Optimal design of an electric power steering system for sport cars. In: 23rd International Symposium on Dynamics of Vehicles on Roads and Tracks, 19–23 Aug Qingdao, China (2013)
28. True, H.: Multiple attractors and critical parameters and how to find them numerically: the right, the wrong and the gambling way. Veh. Syst. Dyn. **51**(3), 443–459 (2013)
29. Liu, Z., Payre, G., Bourassa, P.: Stability and oscillations in a time-delayed vehicle system with driver control. Nonlinear Dyn. **35**, 159–173 (2004)
30. Liu, Z., Payre, G., Bourassa, P.: Nonlinear oscillations and chaotic motions in a road vehicle system with driver steering control. Nonlinear Dyn. **9**, 281–304 (1996)
31. Tang, T., Li, C., Huang, H., Shang, H.: A new fundamental diagram theory with the individual difference of the driver's perception ability. Nonlinear Dyn. **67**, 2255–2265 (2012)
32. Yi-Rong, K., Di-Hua, S., Shu-Hong, Y.: A new car-following model considering driver's individual anticipation behavior. Nonlinear Dyn. **82**, 1293–1302 (2015)
33. Wen, H., Rong, Y., Zeng, C., Qi, W.: The effect of driver's characteristics on the stability of traffic flow under honk environment. Nonlinear Dyn. **84**, 1517–1528 (2016)